The Crop Journal 14 (2026) 1242–1254

Contents lists available at ScienceDirect

The Crop Journal

journal homepage: www.keaipublishing.com/en/journals/the-crop-journal/

MsSGR interacts with MsMSRB5 to antagonistically regulate salt tolerance in *Medicago sativa*

Chun Li [1], Xiaoxia Shen [1], Yulin Jing, Ziyi Hao, Rongchen Yang, Jiahua Wu, Jie An, Peizhi Yang *

College of Grassland Agriculture, Northwest A&F University, Yangling 712100, Shaanxi, China

ARTICLE INFO

Article history:
Received 15 July 2025
Revised 20 March 2026
Accepted 25 March 2026
Available online 18 April 2026

Keywords:
MsSGR
Salt stress
MsMSRB5
Chlorophyll
Alfalfa

ABSTRACT

Photosynthesis is the basis of plant growth and development. It directly influences forage yield and quality; however, salt stress severely inhibits photosynthetic efficiency, accelerates leaf senescence, and reduces alfalfa yield and quality. Stay-green proteins (SGR) are important regulators of chlorophyll degradation and leaf senescence. RT-qPCR analysis of alfalfa seedlings revealed that *MsSGR* expression is significantly induced by salt stress in leaves and roots, suggesting its potential involvement in salt tolerance. Nevertheless, the specific role of MsSGR in the salt stress response of alfalfa remains unclear. We found that MsSGR is a negative regulator of salt tolerance in alfalfa. Compared with wild-type lines, *MsSGR*-overexpression (*MsSGR*-OE) lines exhibited more severe damage to photosynthesis, increased ROS accumulation, reduced antioxidant enzyme activity, and a higher mortality rate. Conversely, the *MsSGR* knockout (*MsSGR*-KO) line showed enhanced salt tolerance and survival rates. RNA-seq analysis revealed that the salt-sensitive phenotype of the *MsSGR*-OE lines was primarily affected by photosynthetic and antioxidant pathways. In addition, yeast two-hybrid, split luciferase complementation, and pull-down assays confirmed an interaction between MsSGR and MsMSRB5. Moreover, chlorophyll degradation assays indicated that MsMSRB5 can inhibit MsSGR-mediated chlorophyll degradation. *MsMSRB5* overexpression significantly improved alfalfa salt tolerance. Based on these findings, we propose a mechanism for alfalfa salt tolerance mediated by the MsSGR-MsMSRB5 molecular module. This study enhances our understanding of how MsSGR regulates alfalfa salt tolerance and provides breeding strategies for developing salt-tolerant alfalfa varieties.

© 2026 Crop Science Society of China and Institute of Crop Sciences, CAAS. Publishing services by Elsevier B.V. on behalf of KeAi Communications Co. Ltd. This is an open access article under the CC BY license (http://creativecommons.org/licenses/by/4.0/).

1. Introduction

Alfalfa is a widely cultivated forage crop; however, its tolerance to salt stress is limited. Soil salinization is a global environmental issue that has experienced a continuous escalation in its extent and severity with the expansion of agricultural cultivation worldwide [1,2]. This constitutes one of the most significant threats to global agricultural production by compromising food security and environmental health. Salt stress causes ionic toxicity, osmotic inactivation, and excessive accumulation of reactive oxygen species (ROS) [3–5]. This further disrupts nutrient absorption, photosynthesis, and antioxidant systems in plants, thus affecting plants at the morphological, physiological, biochemical, and molecular levels [6]. Such disruptions ultimately culminate in reduced yield.

Crop yield is closely linked to photosynthesis, a relationship directly or indirectly affected by photosynthetic efficiency. Chlorophyll content is a key factor that influences photosynthesis. To date, genes encoding all major chlorophyll degradation enzymes have been identified [7–10]. Of these, SGR1 encodes a magnesium dechelatase, which is responsible for the first step in chlorophyll *a* degradation [11]. It is a key gene in the chlorophyll degradation pathway. SGR family proteins may be divided into SGR and SGR-like (SGRL) branches. These proteins regulate chloroplast stability by modulating chlorophyll metabolism and play important roles in senescence and stress adaptation. SGR proteins regulate chlorophyll degradation, thereby influencing leaf senescence and fruit ripening. These processes have been well characterized in *Arabidopsis thaliana* [12], *Oryza sativa* [13], *Lolium perenne* [14], *Cucumis melo* [15], and *Solanum lycopersicum* [16]. During heat stress, the suppression of LpSGR in ryegrass downregulates genes encoding the photosystem proteins and ROS-scavenging enzymes, while upregulating ROS-generating genes, resulting in severe phototoxic damage [14]. Under salt stress, SGR1 and SGRL

* Corresponding author.
E-mail address: yangpeizhi@126.com (P. Yang).
[1] These authors contribute equally to this work.

https://doi.org/10.1016/j.cj.2026.03.016
2214-5141/© 2026 Crop Science Society of China and Institute of Crop Sciences, CAAS. Publishing services by Elsevier B.V. on behalf of KeAi Communications Co. Ltd. This is an open access article under the CC BY license (http://creativecommons.org/licenses/by/4.0/).

synergistically increase chlorophyll degradation in advance of leaf senescence [17]; however, the mechanism underlying the SGR-mediated regulation of plant salt tolerance remains unclear. In alfalfa, *MsSGR* expression is induced in leaves and roots under salt stress. This suggests that this protein may play a key role in mediating the response of alfalfa to salt stress.

Salt stress not only accelerates chlorophyll degradation but also induces excessive production of reactive oxygen species (ROS), leading to oxidative damage to proteins. Methionine sulfoxide reductases (MSRs) reduce methionine sulfoxide (MetO) in proteins and small molecules, thereby mitigating protein oxidative damage [18]. In addition, *MSRs* modulate intracellular signaling pathways by regulating protein oxidation states. They play a role in the oxidative stress response, immune reactions, and seed longevity. Following oxidation, methionine generates S-MetO and R-MetO isomers. Plants have developed two specialized enzyme families, methionine sulfoxide reductase A (MSRA) and methionine sulfoxide reductase B (MSRB), that reduce S-MetO and R-MetO [19–23].

Arabidopsis thaliana contains 5 members of *MSRA* and 9 members of *MSRB* [24]. Maize contains 3 *MSRA* members and 3 *MSRB* members, respectively [25]. Rice contains 4 *MSRA* members and 3 *MSRB* members [26]. Both *MSRs* are related to the tolerance of plants to biotic and abiotic stresses [27,28]. OsMSRA4.1, a chloroplast-localized protein, reduces oxidized methionine in chloroplasts, which ameliorates ROS-induced damage and maintains the integrity and stability of chloroplast membranes during salt stress [26]. Moreover, increased *MSRB* expression under salt stress is closely associated with enhanced antioxidant capacity [29]; however, its interplay with chlorophyll regulation remains unclear.

In this study, we demonstrated that *MsSGR*-OE inhibits the photosynthetic and antioxidant pathways of alfalfa during salt stress, leading to salt sensitivity. Conversely, *MsSGR* knockout significantly enhances the salt tolerance of alfalfa. We identified MsMSRB5 as an interacting protein of MsSGR, and both proteins are localized to the chloroplast, plasma membrane, and nucleus. MsMSRB5 inhibits chlorophyll degradation by MsSGR and positively regulates alfalfa salt tolerance. These results indicate that the MsSGR-MsMSRB5 module affects alfalfa salt tolerance by attenuating chlorophyll metabolism and cellular redox homeostasis. Our results provide new insights into the regulatory mechanisms underlying SGR protein-mediated plant responses to abiotic stress and offer potential targets for improving stress resistance in crops.

2. Materials and methods

2.1. Plant materials and growth conditions

In this study, *Medicago sativa* cv. Xinjiang DaYe was used as the material for gene expression analysis. To investigate the expression patterns of *MsSGR* and *MsMSRB5* in multiple tissues, roots, young leaves, old leaves, stems, and flowers of alfalfa grown under normal conditions in an incubator were collected. For studying the expression patterns of *MsSGR* and *MsMSRB5* under salt stress, alfalfa seedlings were grown in Hoagland nutrient solution under long-day (LD) conditions with a photoperiod of 16 h light (180 μmol m^{-2} s^{-1}) and 8 h darkness, at a temperature of 22 °C and a relative humidity of 70%. The nutrient solution was replaced every 4 d during the growth period. During seedling growth, the nutrient solution was replaced every 4 d. Two-week-old alfalfa seedlings were divided into two groups. For the first group, the seedlings were exposed for 24 h to Hoagland solution containing various concentrations of NaCl (0, 50, 100, 150, 200, and 250 mmol L^{-1}). For the second group, the seedlings were exposed to Hoagland solution containing 200 mmol L^{-1} NaCl for various exposure times (0, 1, 3, 6, 9, 12, and 24 h). Each treatment included three biological replicate samples. All samples were immediately frozen in liquid nitrogen for RNA preparation.

2.2. Vectors construction and plant transformation

For the construction of overexpression (OE) vectors, the recombinant pCAMBIA1300-35S: *MsSGR* and pCAMBIA1300-35S: *MsMSRB5* plasmid constructs were generated using, respectively, the full-length coding sequence of *MsSGR* and *MsMSRB5* amplified from alfalfa cultivar Xinjiang DaYe. The *Agrobacterium tumefaciens* EHA105 strain carrying the construct pCAMBIA1300-35S: *MsSGR* and pCAMBIA1300-35S: *MsMSRB5* was used to transform *Medicago sativa* cv. Xinjiang DaYe. We used a CRISPR/Cas9 construct to knock out the *MsSGR* gene. The gRNAs targeting *MsSGR* were designed using the CRISPR RGEN Tools (http://www.rgenome.net/cas-designer/). The sequences of the gRNA1: 5′-TTCCAAATAGAA GACGGTTATGG-3′ and gRNA2: 5′-ATTGATGAAGACAAACATC CAGG-3′. Similarly, the *A. tumefaciens* EHA105 strain carrying the construct pCas9-sgMsSGR was used to transform Xinjiang DaYe.

2.3. Biomass and relative water content (RWC)

The aboveground parts of wild-type (WT) and transgenic plants treated under control and salt stress conditions were collected. After determining the fresh weight (FW) of the aboveground parts, samples were blanched at 105 °C for 20 min and then dried at 65 °C to constant weight to measure dry weight (DW). For RWC determination, after measuring fresh weight (Wf), plants were immersed in distilled water until saturated, stored at 4 °C overnight, dried by blotting surface moisture, and then weighed for turgid weight (Wt). Samples were subsequently dried at 65 °C to constant weight for dry weight (Wd) measurement. RWC was calculated as: RWC = (Wf – Wd) / (Wt – Wd). Each treatment was replicated three times.

2.4. Measurement of POD, SOD, MDA, Pro, H_2O_2 and pigment

Plants were irrigated with 200 mmol L^{-1} or 400 mmol L^{-1} NaCl every 3 d for 7 consecutive days. Activities of peroxidase (POD) and superoxide dismutase (SOD), as well as contents of malondialdehyde (MDA), proline (Pro), and hydrogen peroxide (H_2O_2) were determined using corresponding detection kits (BC0095, BC0175, BC3595, BC0295, and BC0025, respectively; Solarbio, Beijing, China), with parameters measured via a microplate reader. Additionally, leaf samples were stained with NBT solution, incubated at room temperature for 24 h, decolorized in 80% ethanol, and photographed. After salt stress, chlorophyll was extracted overnight in 96% ethanol in the dark. Following centrifugation, the supernatant was collected, and absorbance was measured using a microplate reader. Contents of chlorophyll *a*, chlorophyll *b*, carotenoids, and total chlorophyll were calculated based on absorbance values at 665 nm, 649 nm, and 470 nm.

2.5. Rna-seq analysis

The leaves of WT and *MsSGR*-OE (#9, #10) alfalfa lines treated with 0 and 200 mmol L^{-1} NaCl were used for RNA-seq. Three biological replicates were conducted on each group of samples. RNA-seq and subsequent analysis were conducted by BMKCloud (https://www.biocloud.net). To validate the differentially expressed genes identified by RNA sequencing, 12 genes were selected for relative expression analysis via RT-qPCR. The primers used are listed in Table S1.

2.6. Y2H assay

The full-length sequence of *MsSGR* was cloned into the pGBKT7 vector (Table S1). The recombinant plasmid was co-transformed

with the alfalfa pGADT7 library plasmid into the yeast strain AH109 for library screening. The alfalfa cDNA library was constructed by Nanjing Ruiyuan Biotechnology Co., Ltd. The construction material was a mixture of different tissues (including leaves, stems, and roots) of *Medicago sativa* cv. XinJiang Daye. The detailed protocol was as follows: first, total RNA was extracted, and mRNA was purified. Subsequently, cDNA was synthesized, and the obtained cDNA was normalized to balance transcript abundance and remove short fragments. Finally, the cDNA was cloned into the linearized pGADT7 vector via homologous recombination. The constructed plasmid library was transformed into *E. coli* Top10 for amplification, and after passing quality verification, large-scale plasmid extraction was performed.

Co-transformation of pGADT7 and pGBKT7-*MsSGR* served as a negative control. The transformants were spread on SD/-Trp/-Leu plates and cultured at 30 ℃. Successfully transformed single clones were picked and spotted onto SD/-Trp-Leu-His-Ade plates. After positive colonies emerged, they were sequenced, and interacting protein information was obtained by alignment in NCBI. The full-length sequence of *MsMSR* was cloned into the pGADT7 vector and co-transformed with pGBKT7-*MsSGR*. Positive clones were screened by growth on SD/-Ade/-His/-Leu/Trp/+3AT/+x-α-gal medium.

2.7. Split-luc assay

The full-length *MsSGR* sequences were cloned into the N-terminus encoding regions, and the full-length *MsMSRB*5 sequences were cloned into the C-terminus encoding regions of the luciferase, respectively [30]. These constructs were co-infiltrated into *Nicotiana benthamiana*, and the infiltrated leaves were analyzed for LUC activity at 48 h after infiltration using the Multispectral Dynamic Fluorescence Microscopy System (PlantView100).

2.8. Pull-down assay

The coding sequences of the *MsSGR* and *MsMSRB5* genes were respectively cloned into the pGEX-4 T-1 and pclod-TF vectors. The primer sequences are shown in Table S1. Then, the vectors were transformed into the *Escherichia coli* strain DE3. After induction, the cells were lysed, and the proteins were extracted and purified. Referring to the GST Protein Interaction Pull-Down Kit, the purified proteins were added and incubated overnight at 4 °C. After elution, the proteins were detected by Western blot.

2.9. Subcellular localization of MsSGR and MsMSRB5

The CDS sequences of *MsSGR* and *MsMSRB5* were fused to GFP and mCherry, respectively, to generate the vectors pCAMBIA1300-35S: *MsSGR*-GFP and pCAMBIA2302-35S: MsMSRB5-mCherry. Using 35S: GFP and 35S: mCherry as control vectors, all constructs were transformed into *Agrobacterium tumefaciens* strain GV3101. *Agrobacterium* was cultured to an OD_{600} of 0.8, and the bacterial pellets were resuspended in infiltration buffer to a final OD_{600} of 0.6, 1.2, and 1.8, respectively. Mix at a 1:1 volume ratio and infiltrate into tobacco leaves. After 1 d, plants were treated with 200 mmol L^{-1} NaCl, followed by photography and determination of chlorophyll content at 3 d of treatment. Epidermal cells were observed under a laser confocal scanning microscope.

2.10. MsMSRB genes identification and chromosomal mapping

The genomic data of Xinjiang DaYe were downloaded from the figshare database (https://figshare.com/articles/dataset/Medicago_sativa_genome_and_annotation_files/12623960). Using the protein sequences of the *MSRB* gene family from Arabidopsis as templates, blast alignment was performed against the alfalfa genome protein sequences to obtain potential members. After screening and correction, the MSRB family protein sequences of alfalfa were obtained. The TBtools software [31] was used to predict the molecular weight (Mw), isoelectric point (pI), and average hydrophilicity of alfalfa MSRB proteins, and to visualize the position information of MSRB obtained from the alfalfa gene annotation file. The subcellular localization was predicted using the WolF PSORT website (https://wolfpsort.hgc.jp/).

2.11. Analysis of MsMSRB gene structure and motif composition

The protein sequences of the MsMSRB gene family were submitted to the MEME website (https://meme-suite.org/meme/tools/meme) for conserved motif analysis, and the number of motifs was set to 10. The gene structure information of *MsMSRB* was extracted from the alfalfa genomic annotation file, and the conserved motifs of proteins and the gene structures were visualized using the TBtools software.

2.12. Phylogenetic analysis of MsMSRB

Phylogenetic analysis was performed using MEGA11 software [32]. The maximum likelihood (ML) method, with the Jones-Taylor-Thornton (JTT) model, was applied to construct a phylogenetic tree based on the protein sequences of the *Arabidopsis* MSRB family and the obtained alfalfa MSRB family. Additionally, using the protein sequence of MsMSRB5 as a template, a BLAST search was conducted in NCBI to obtain homologous sequences of MsMSRB5 from other species, followed by multiple sequence alignment.

2.13. Real-time quantitative PCR (RT-qPCR) analysis

Total RNA was extracted from the samples using the Eastep Super Total RNA Extraction Kit (Promega Biotech, Shanghai, China). The total RNA was reverse transcribed as cDNA using HiScript III RT SuperMix for qPCR (with gDNase) (Vazyme Biotech, Nanjing, Jiangsu, China). Gene-specific primers for RT-qPCR are listed in Table S1. qPCRs were performed using ChamQ SYBR qPCR master mix (Vazyme Biotech) in a 96-well real-time PCR system (LightCycler 480 II, Roche, Switzerland), and the procedure was as follows: 95 °C for 30 s, 40 cycles of 95 °C for 5 s, and 60 °C for 30 s. Three technical replicates were performed for each sample. The expression levels of each gene were normalized to those of *MsACTIN*, and relative gene expression levels were calculated by the $2^{-\Delta\Delta CT}$ method.

2.14. Statistical analysis

One-way ANOVA or two-way ANOVA was performed, followed by Fisher's LSD test, to determine the significance of the difference (*, $P < 0.05$; **, $P < 0.01$; ***, $P < 0.001$). GraphPad Prism 8.0.1 was used to draw the graphs and perform the statistical tests.

3. Results

3.1. MsSGR is regulated by salt stress and localized to chloroplasts, nuclei, and cell membranes

To determine the expression profile of *MsSGR*, we measured its expression in various organs of *Medicago sativa* (Fig. S1A). The results indicated that under normal conditions, *MsSGR* was predominantly expressed in old leaves, petioles, and flowers, with the highest expression in old leaves and the lowest in young leaves.

Following treatment with 200 mmol L^{-1} NaCl for 6 h, *MsSGR* expression was downregulated in alfalfa old leaves and petioles, whereas it was upregulated in flowers. To determine the role of *MsSGR* in salt stress in alfalfa, RT-qPCR was used to measure the expression pattern of *MsSGR* under salt stress. First, we measured the expression of *MsSGR* in alfalfa leaves treated with various salt concentrations for 24 h (Fig. S1B). The results indicated that *MsSGR* expression was induced by high concentrations (200 and 250 mmol L^{-1}) of salt, with the highest levels observed at 250 mmol L^{-1}. In addition, at 200 mmol L^{-1} NaCl, the expression of *MsSGR* in the leaves increased significantly from 1 to 24 h, peaked at 12 h, and decreased slightly at 24 h (Fig. S1C). In roots, *MsSGR* expression increased significantly from 3 to 24 h, reached its highest level at 9 h, and began to decrease at 12 h (Fig. S1D). Finally, subcellular localization assays revealed that MsSGR is localized to the chloroplasts, nuclei, and cell membranes (Fig. S1E).

3.2. Overexpression of MsSGR in alfalfa confers sensitivity to salt stress

To identify the function of *MsSGR* during the salt response, *MsSGR* was overexpressed in alfalfa, and PCR assays were performed on genomic DNA using primers specific to the Basta resistance gene (*BlpR*). The results indicated that the expected *BlpR* fragment was successfully amplified in all 10 overexpressing lines, confirming the stable integration of the *MsSGR* cassette into the plant genome (Fig. S2). Next, two lines exhibiting high expression levels (OE #9 and OE #10) were selected from the positive OE plants with significant expression differences compared with the WT to evaluate salt tolerance (Fig. 1A). First, 40-d-old plants showing consistent growth were treated with 200 mmol L^{-1} NaCl. After 7 d, the leaves of the *MsSGR*-OE lines exhibited distinct yellowing, which was in contrast to the phenotype of the WT plants (Fig. 1B). Compared with the WT, the fresh weight (Fig. 1C), dry weight (Fig. 1D), relative water content (Fig. 1E), chlorophyll *a* and *b* contents (Fig. 1F), and carotenoid content (Fig. 1G) of the OE lines were significantly decreased. These results indicate that increased *MsSGR* expression results in salt sensitivity in alfalfa.

Next, we determined the effect of *MsSGR* overexpression on photosynthesis in alfalfa under salt stress. Following treatment with 200 mmol L^{-1} NaCl, the F_v/F_m (maximum photochemical efficiency) values of the overexpression plants decreased significantly, whereas those in the WT remained unchanged (Fig. 2A, B). The Y(II) (actual photochemical efficiency) values for the *MsSGR*-OE plants showed a marked decrease compared with those in the WT plants following salt treatment (Fig. 2C, D).

The NPQ/4 value for the MsSGR-OE lines decreased by approximately 50% compared with that in the control following NaCl treatment, whereas no significant difference was observed in the WT plants (Fig. 2E, F). Under NaCl treatment, the Y(NO) values for the *MsSGR*-OE lines were higher compared with those in the WT (Fig. 2G, H). In addition, the q_N values for the WT plants were significantly higher compared with those of the *MsSGR*-OE lines (Fig. 2I, J). Following treatment with 200 mmol L^{-1} NaCl, the ETR values of the WT decreased by approximately 22%, whereas the *MsSGR*-OE plants showed a significant decrease, with 36% in OE #9 and 38% in OE #10 (Fig. 2K).

Following salt treatment, H_2O_2 content, NBT staining intensity (an indicator of ROS levels), and MDA levels were significantly higher in the *MsSGR*-OE lines compared with those in the WT plants (Fig. 3A–C). Salt stress increased the level of osmolyte Pro, with *MsSGR*-OE plants exhibiting significantly higher Pro content compared with the WT plants (Fig. 3D). POD and SOD activity were measured to determine the effect of salt stress on antioxidant enzymes in WT and OE plants. The POD and SOD activities of these two enzymes in OE plants were significantly lower compared with those in WT plants after salt stress (Fig. 3E, F).

3.3. Rna-seq analysis of sensitive alfalfa by MsSGR-OE

To determine the basis for salt sensitivity in alfalfa by MsSGR, an RNA-seq assay was performed. *MsSGR*-OE (#9, #10) and WT leaves were used for RNA-seq analysis at 0 and 200 mmol L^{-1} NaCl treatment. Principal component analysis (PCA) was performed on all samples, and the results indicated a strong clustering effect (Fig. S3A). At 0 and 200 mmol L^{-1} NaCl treatment, compared with the WT, 4774 and 6024 upregulated genes and 8201 and 9735 downregulated genes were identified in OE9, respectively, whereas 3655 and 4978 upregulated genes and 6188 and 8671 downregulated genes were identified in OE10 (Fig. S3B).

KEGG enrichment analysis of these differentially expressed genes (DEGs) revealed that without NaCl stress, the DEGs between the OE lines and the WT were primarily enriched in ribosome, as well as valine, leucine, and isoleucine degradation and glutathione metabolism (Fig. S3C–F). Following 200 mmol L^{-1} NaCl treatment, the DEGs between OE and WT were also enriched in arginine and proline metabolism, peroxisome, and carotenoid biosynthesis. This suggests that MsSGR regulates alfalfa salt tolerance through these pathways (Fig. S3E, F).

We performed a heatmap analysis and observed that the majority of genes mapped to the glutathione metabolism pathway (ko00480) and peroxisome pathway (ko04146) were significantly downregulated (Fig. 4A, B), which was consistent with the reduced antioxidant enzyme activities and enhanced ROS accumulation observed. Considering the severe inhibition of photosynthesis during salt stress, we analyzed DEGs associated with photosynthesis (ko00195), photosynthesis-antenna proteins (ko00196), and carotenoid biosynthesis (ko00906). Most of the key genes in these processes were markedly downregulated in OE lines (Fig. 4C), which is consistent with the decreased photosynthetic efficiency at the transcriptional level.

RT-qPCR assays confirmed that the transcript levels of the antioxidant genes (SOD, POD, APX) and photosynthesis-related genes (PSI, PSII, and antenna proteins) were significantly lower in OE lines compared with those in the WT following salt treatment (Fig. 4D–O). Taken together, these results indicate that MsSGR overexpression suppresses photosynthetic and antioxidant pathways at the transcriptional level, thus exacerbating salt sensitivity in alfalfa.

3.4. MsSGR knockout improves the physiological parameters of transgenic alfalfa following salt stress treatment

The effects of *MsSGR* knockout on salt tolerance in alfalfa were examined. Initially, the effect of 200 mmol L^{-1} NaCl on *MsSGR*-KO plants was determined; however, no significant differences were observed between *MsSGR*-KO and WT plants after 200 mmol L^{-1} NaCl treatment for 7 d. Therefore, the phenotypic changes of *MsSGR*-KO plants under 400 mmol L^{-1} NaCl stress were examined. After one week of treatment, the growth of WT plants was inhibited, with some leaves turning white and wilting (Fig. S4A, B). The fresh and dry weight of the plants significantly decreased following salt treatment, with a more pronounced reduction in WT plants (Fig. S4C, D). The relative water content of the WT plants decreased significantly (Fig. S4E). In addition, we observed that OE plants began to exhibit leaf yellowing 2 d after treatment with 400 mmol L^{-1} NaCl. The plant mortality rate was calculated 14 d after treatment (Fig. S4F). The mortality rate of the WT plants (54.67%) was significantly lower compared with that of OE #9 (82.78%) and OE #10 (90%), and significantly higher compared with that of *MsSGR*-KO (23.16%). The results indicate that *MsSGR*-KO enhances plant salt tolerance.

Following salt treatment, the chlorophyll *a* (Fig. S4G), chlorophyll *b* (Fig. S4H), and carotenoid (Fig. S4I) content in the *MsSGR*-

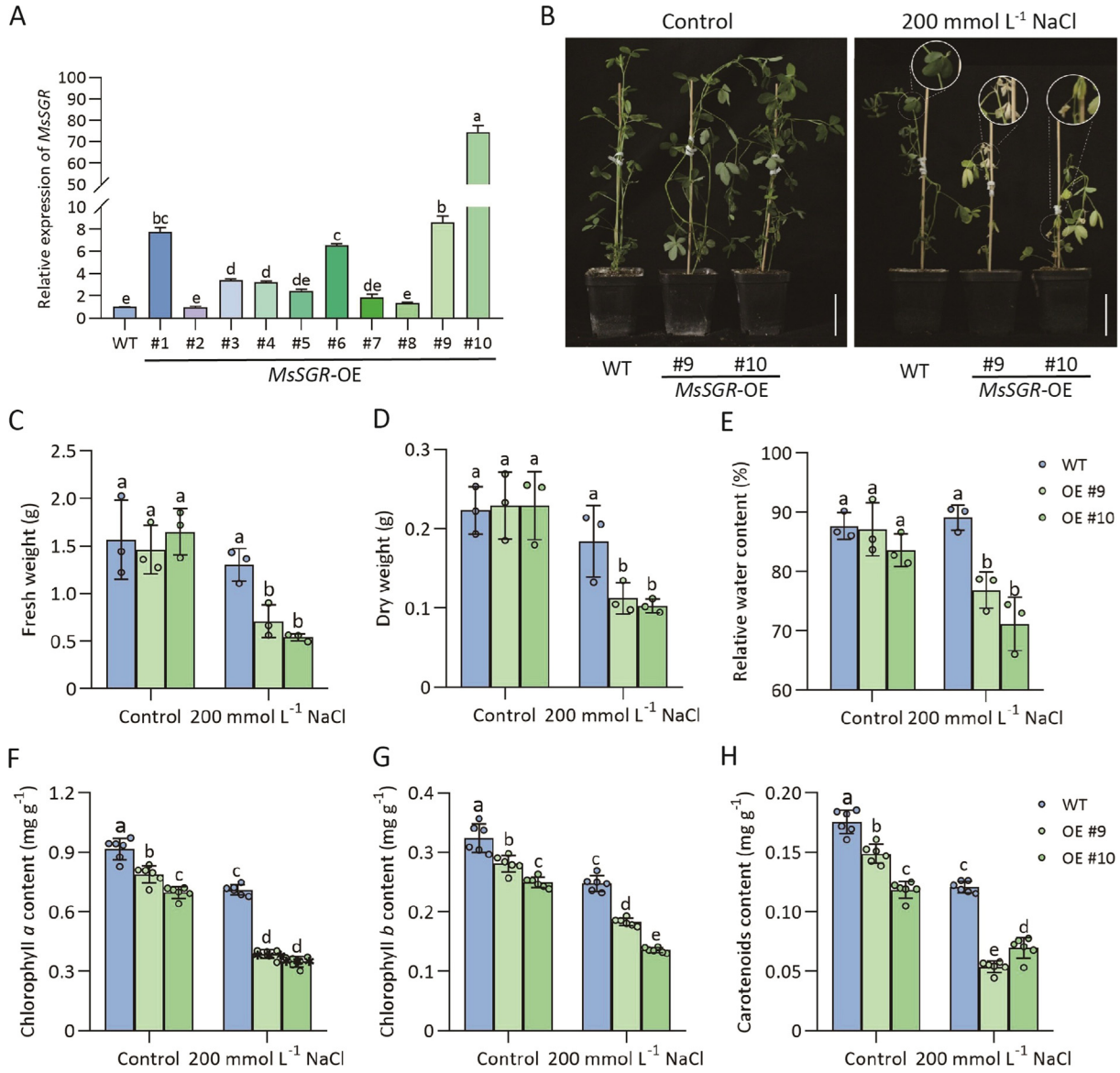


Fig. 1. *MsSGR*-OE plays a negative role in alfalfa salt resistance. (A) Expression of *MsSGR* in plants. Error bars indicate SD (n = 3). One-way ANOVA, with statistically significant differences at $P < 0.05$. (B) Salt treatment of *MsSGR*-OE plants. The cuttings of WT and *MsSGR*-OE plants were inserted into vermiculite and cultured for 40 d, then treated with 200 mmol L^{-1} NaCl solution irrigated every two d for one week. The control group was irrigated with the same volume of nutrient solution without NaCl. (C) Shoot fresh weight of plants under 200 mmol L^{-1} NaCl for 7 d. (D) Shoot dry weight of plants under 200 mmol L^{-1} NaCl for 7 d. (E) Shoot relative water content. Error bars indicate SD (n = 3). (F) Leaf chlorophyll *a* content under 200 mmol L^{-1} NaCl for 7 d. (G) Leaf chlorophyll *b* content under 200 mmol L^{-1} NaCl for 7 d. (H) Leaf carotenoid content under 200 mmol L^{-1} NaCl for 7 d. Error bars indicate SD (n = 6). WT, wild-type alfalfa; OE, overexpression of *MsSGR* transgenic alfalfa. Bars labeled with different letters indicate significant differences between groups, while bars with the same letter show no significant differences (Two-way ANOVA, Fisher's LSD test, $P < 0.05$).

KO lines was significantly higher compared with those in WT plants. After treatment with 400 mmol L^{-1} NaCl, the F_v/F_m values for the WT plants decreased significantly (Fig. S5A, B), and the Y (II) values of *MsSGR*-KO were significantly higher compared with those of the WT (Fig. S5C, D), suggesting a higher actual photosynthetic efficiency in *MsSGR*-KO. The NPQ/4 values for the *MsSGR*-KO plants increased significantly (Fig. S5E, F), indicating that *MsSGR*-KO plants convert light energy more efficiently into heat. The Y (NO) values for *MsSGR*-KO were significantly lower compared with those of the WT (Fig. S5G, H), whereas the q_N values were significantly higher (Fig. S5I, J). After salt treatment, the ETR for the WT plants decreased by approximately 44%, whereas the ETR values of the *MsSGR*-KO lines showed no significant change (1%); however, the rate of increase was reduced (Fig. S5K). These results indicate that *MsSGR*-KO may reduce the degree of light damage and enhance the photosynthetic capacity of alfalfa during salt stress.

MsSGR-KO plants also exhibited lower NBT staining levels after salt treatment (Fig. S6A), with significantly reduced H_2O_2, MDA, and Pro content in the leaves (Fig. S6B–D), and significantly higher POD and SOD activity compared with the WT plants (Fig. S6E, F). These results indicate that *MsSGR*-KO reduces cellular damage and enhances plant salt tolerance by decreasing MDA, Pro, and H_2O_2 accumulation and increasing antioxidant enzyme activities under salt stress.

3.5. MsMSRB5 interacts with MsSGR and inhibits the chlorophyll degradation activity of MsSGR

To elucidate the underlying mechanism by which *MsSGR* affects salt tolerance in alfalfa, a yeast two-hybrid (Y2H) system was used to identify interacting proteins. No self-transcriptional activation was detected for the full-length MsSGR protein (Fig. S7). Using

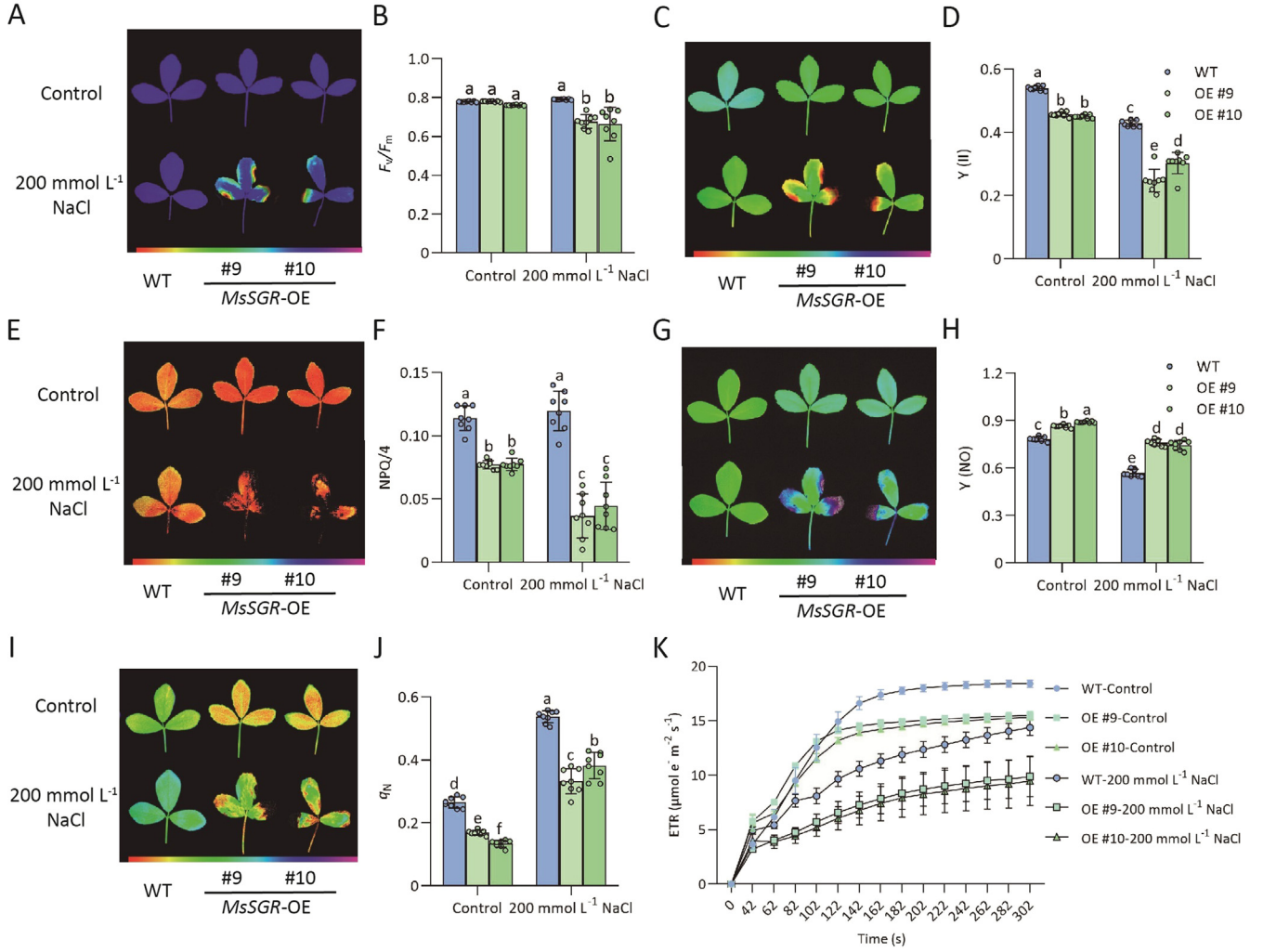


Fig. 2. *MsSGR*-OE can affect photosynthesis in alfalfa under salt stress. (A) Fluorescence imaging of F_v/F_m in alfalfa. (B) F_v/F_m. (C) Fluorescence imaging of Y(II) in alfalfa. (D) Y (II). (E) Fluorescence imaging of Y(NPQ/4) in alfalfa. (F) Y(NPQ)/4. (G) Fluorescence imaging of Y(NO) in alfalfa. (H) Y(NO). (I) Fluorescence imaging of q_N in alfalfa. (J) q_N. (K) Fluorescence imaging of Electron transport rate (ETR) in alfalfa. Plants were inserted into vermiculite and cultured for 40 d, then treated with 200 mmol L^{-1} NaCl solution irrigated every two d for one week. The control group was irrigated with the same volume of nutrient solution without NaCl. WT, wild-type alfalfa; OE, overexpression of *MsSGR* transgenic alfalfa. Values are means ± SD (n = 8). Bars labeled with different letters indicate significant differences between groups, while bars with the same letter show no significant differences (Two-way ANOVA, Fisher's LSD test, $P < 0.05$).

pGBKT7-*MsSGR* as bait, a Y2H screen was conducted against an alfalfa cDNA library to identify potential interacting proteins. A total of 98 proteins were identified, including the NYC1, MSRB5, and MYB transcription factors, and the ATP synthase 6 kDa subunit. We selected proteins related to biological stress resistance and photosynthesis and verified their interactions using a yeast two-hybrid assay (Fig. S8). Based on the split-luciferase (Split-Luc) assay data (Fig. S9), MSRB was selected as a candidate protein.

To further characterize this potential interacting protein, we analyzed the MsMSRB gene family. Based on the alfalfa genome and the NCBI database, a total of 11 MsMSRB family members were identified and designated MsMSRB1 through MsMSRB11 based on their chromosomal locations (Fig. S10). We constructed an unrooted phylogenetic tree using MsMSRBs and Arabidopsis MSRBs to reveal their evolutionary relationships. As shown in Fig. S12, the MSRB proteins were separated into five clusters (Groups I–V). Group IV contained alfalfa and *Arabidopsis* members, suggesting a close evolutionary relationship, whereas Groups II and III were alfalfa specific (Fig. S11). The MsMSRB family contains three conserved domains: MsrB, PRK03562 superfamily, and SelR, whereas MsMSRB5 only retains the MSRB domain (Fig. S12). Multiple sequence alignment revealed a conserved region in all of the MSRB5 proteins (Fig. S13; protein sequences in Table S2). MsMSRB5 shared the highest similarity (93%) with *Medicago truncatula* Medtr4g092800 and was evolutionarily closer to legumes, but distant from gramineous and cruciferous plants (Fig. S14).

MS.gene90268, located on chromosome chr4.2, was designated *MsMSRB5* (Table S3). *MsMSRB5* is 3384 bp in length and contains 3 exons and 2 introns, with a 594 bp open reading frame (ORF) encoding 198 amino acids and a conserved MSRB domain (Fig. S15; Table S4). Co-expression of *MsSGR*-nLuc and cLuc-*MsMSRB5* resulted in significant luminescence signals, whereas the control groups showed minimal signal (Fig. 5A), confirming that MsSGR and MsMSRB5 can form a stable protein complex in planta. Pulldown assays further confirmed a direct interaction between MsSGR and MsMSRB5 (Fig. 5B). Subcellular localization experiments revealed that MsMSRB5 and MsSGR were co-localized to chloroplasts, nuclei, and plasma membrane (Fig. 5C, D). Further functional assays indicated that MsMSRB5 inhibits MsSGR mediated chlorophyll degradation. When co infiltrated with high concentrations of MsMSRB5 (OD_{600} = 1.2 or 1.8), the chlorophyll content was significantly increased (Fig. 6A, B). Under

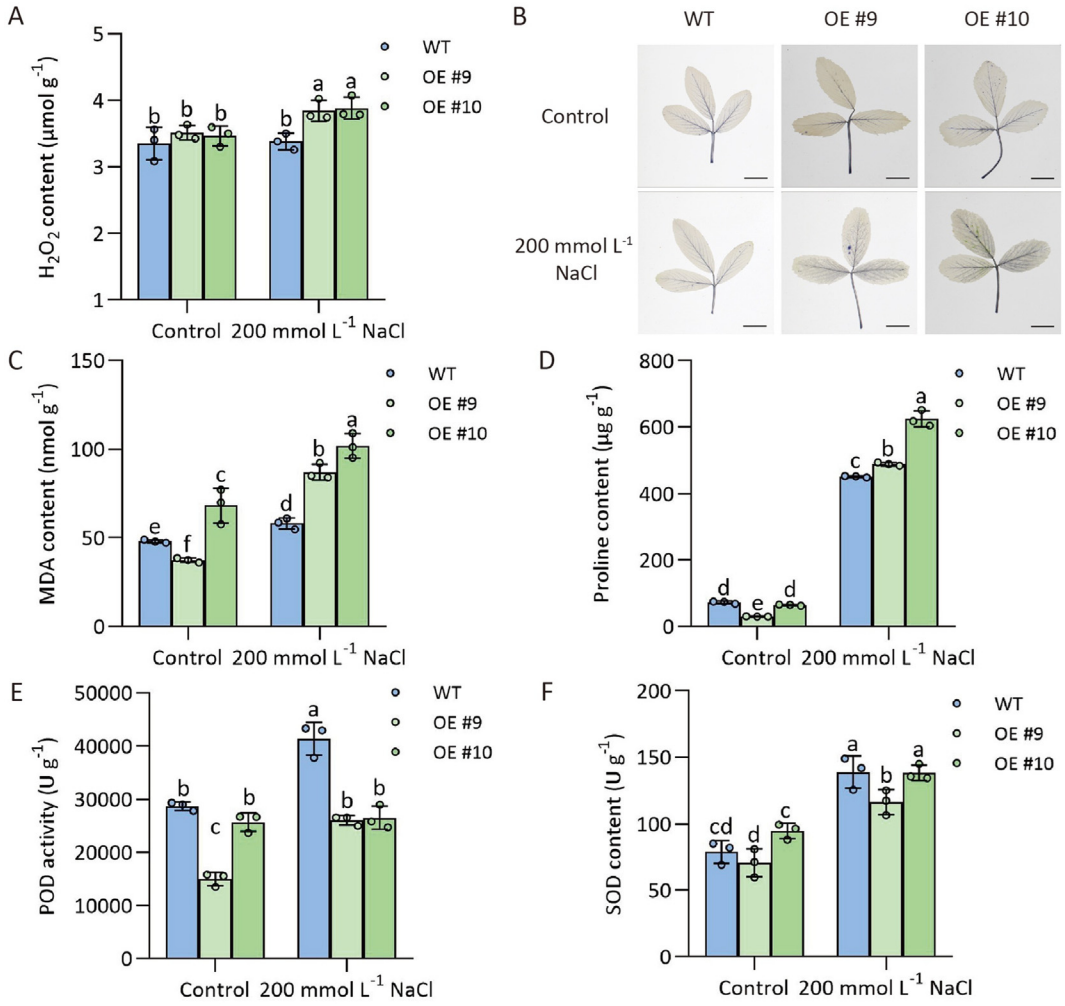


Fig. 3. *MsSGR*-OE promotes the accumulation of ROS and inhibits the activity of active oxygen scavenging enzymes in alfalfa under salt stress. (A) Alfalfa leaf H_2O_2 content. (B) Alfalfa leaf DAB staining. (C) Alfalfa leaf MDA content. (D) Alfalfa leaf proline content; (E) Alfalfa leaf POD activity. (F) Alfalfa leaf SOD activity. Alfalfa treatment with 200 mmol L^{-1} NaCl solution irrigated every two d for one week. The control group was irrigated with the same volume of nutrient solution without NaCl. WT, wild-type alfalfa; OE, overexpression of *MsSGR* transgenic alfalfa. Values are means ± SD (n = 3). Bars labeled with different letters indicate significant differences between groups, while bars with the same letter show no significant differences (Two-way ANOVA, Fisher's LSD test, $P < 0.05$).

200 mmol L^{-1} NaCl treatment, leaves co expressing MsMSRB5 and MsSGR retained significantly higher chlorophyll contents and stronger chloroplast autofluorescence compared with those expressing MsSGR alone (Fig. 6C–F). Taken together, MsMSRB5 directly interacts with MsSGR to prevent the chlorophyll degradation of MsSGR, thereby maintaining chlorophyll stability during salt stress.

3.6. *MsMSRB5* overexpression enhances salt tolerance in alfalfa

To determine whether MsMSRB5 functions similarly to MsSGR, RT-qPCR analysis revealed that *MsMSRB5* was primarily expressed in old leaves (Fig. S16A). In leaves treated with 100 mmol L^{-1} NaCl for 24 h, *MsMSRB5* expression was induced to its highest level (Fig. S16B). In leaves, *MsMSRB5* expression was upregulated following treatment with 200 mmol L^{-1} NaCl for 1, 3, 6, and 9 h (Fig. S16C). In contrast, in roots, *MsMSRB5* expression was only induced at 6 h following treatment with 200 mmol L^{-1} NaCl (Fig. S16D).

To characterize the function of MsMSRB5 under salt stress, we overexpressed *MsMSRB5* in alfalfa. RT-qPCR analysis revealed nine independent OE-positive plants with varying mRNA expression of the transgene (Fig. S17). Two typical OE lines (OE #5 and OE #8) with high *MsMSRB5* expression were selected for further evaluation. Under normal conditions, *MsSGR* expression exhibited a decreasing trend in the *MsMSRB5*-OE lines (OE#5, OE#8) compared with the WT plants. Treatment with 400 mmol L^{-1} NaCl inhibited plant growth, causing leaf yellowing in the WT plants, whereas *MsMSRB5*-OE plants showed no obvious phenotypic changes (Fig. 7A), indicating that *MsMSRB5* overexpression enhances alfalfa salt tolerance. Chlorophyll *a*, *b*, and carotenoid content were measured following salt treatment. *MsMSRB5* overexpression significantly increased chlorophyll levels during salt stress (Fig. 7C–E). In addition, the detached leaves were treated with nutrient solutions containing 0, 100, or 200 mmol L^{-1} NaCl for 10 d. The WT leaves exhibited more severe yellowing compared with *MsMSRB5*-OE leaves at the same salt concentration (Fig. 7B), further confirming that *MsMSRB5*-OE improves salt tolerance in alfalfa.

4. Discussion

Salt stress accelerates plant senescence by inducing oxidative stress, disrupting osmotic balance, and inhibiting photosynthesis [33]. SGR directly regulates the rate of chlorophyll degradation, thus affecting plant senescence [34] and playing an important role in plant stress responses [14]. In the present study, we found that

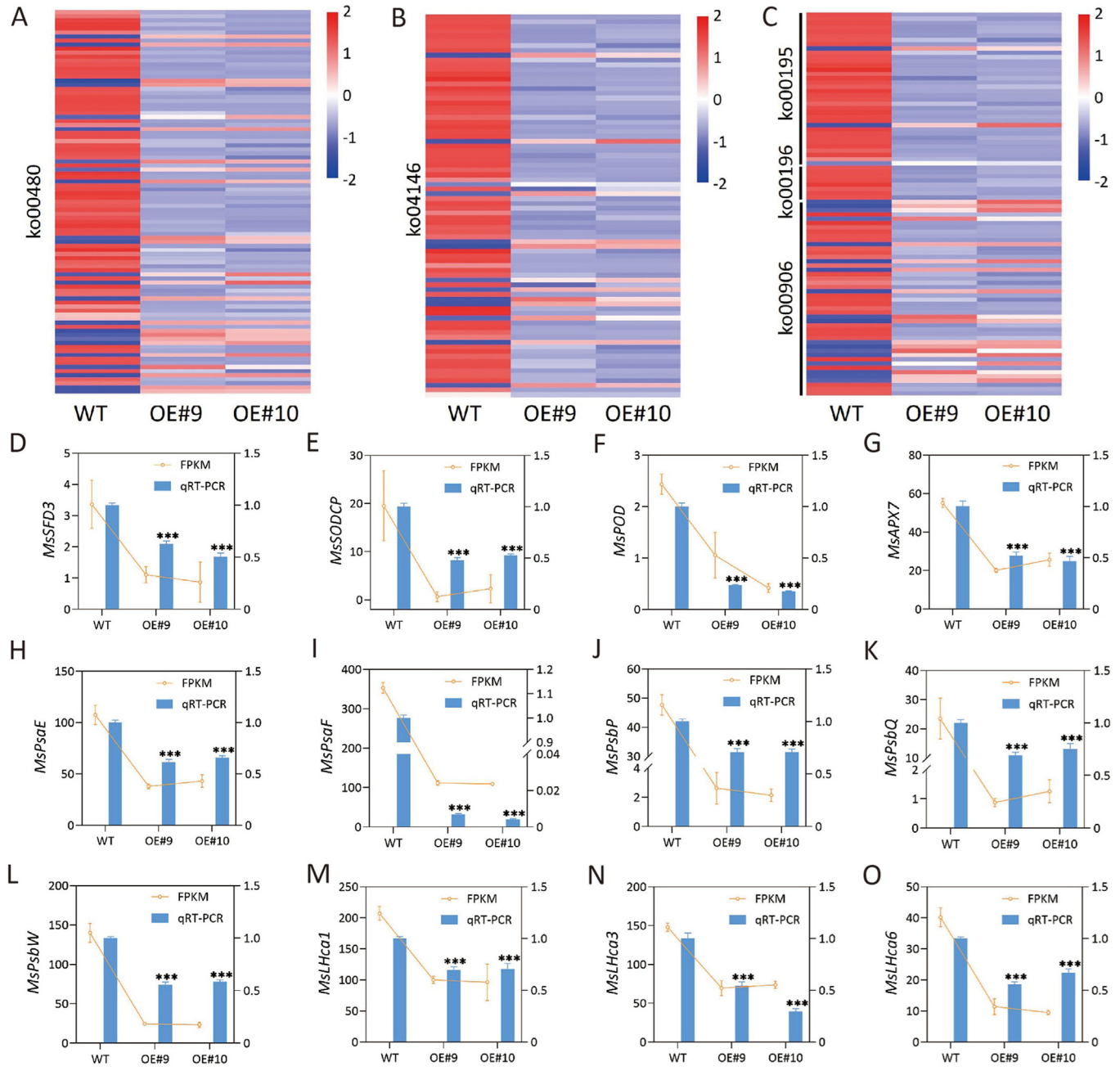


Fig. 4. DEGs analysis and RNA-seq data validation of antioxidant and photosynthetic pathways. (A, B) Heatmap displaying DEGs annotated to the 00480 (Glutathione metabolism) and 04146 (Peroxisome) pathways. (C) Heatmap displaying DEGs annotated to the 00195 (Photosynthesis), 00196 (Photosynthesis-antenna proteins), and 00906 (Carotenoid biosynthesis) pathways. (D–O) RNA-seq profiles and relative expression levels of SOD (D, E), POD (F), ascorbate peroxidase (APX) (G), photosystem I (PSI) (H, I), photosystem II (PSII) (J–L), and photosynthetic antenna proteins (M–O) in alfalfa leaves post NaCl treatment. Values are means ± SE (n = 3). *, $P < 0.05$; **, $P < 0.01$; ****, $P < 0.0001$.

MsSGR exhibits higher expression in old leaves compared with other tissues, and salt treatment significantly inhibits its expression in old leaves (Fig. S1A). Old leaves are key organs for plants to redistribute energy in response to salt stress. High basal *MsSGR* expression in old leaves may facilitate senescence regulation in these tissues. Downregulating *MsSGR* during NaCl treatment likely serves as an adaptive mechanism for alfalfa to avoid excessive senescence of old leaves. Therefore, *MsSGR* may represent a novel component that mediates salt tolerance in alfalfa.

4.1. MsSGR modulates chlorophyll degradation and photosynthesis in alfalfa under salt stress

Chlorophyll content serves as a key indicator for evaluating plant senescence and salt tolerance. Previous studies have demonstrated that *SGR* overexpression accelerates the cascade of chlorophyll degradation and impairs plant photosynthesis [35,36]. Consistent with these findings, the present study shows that *MsSGR*-OE reduced the contents of chlorophyll in alfalfa under salt

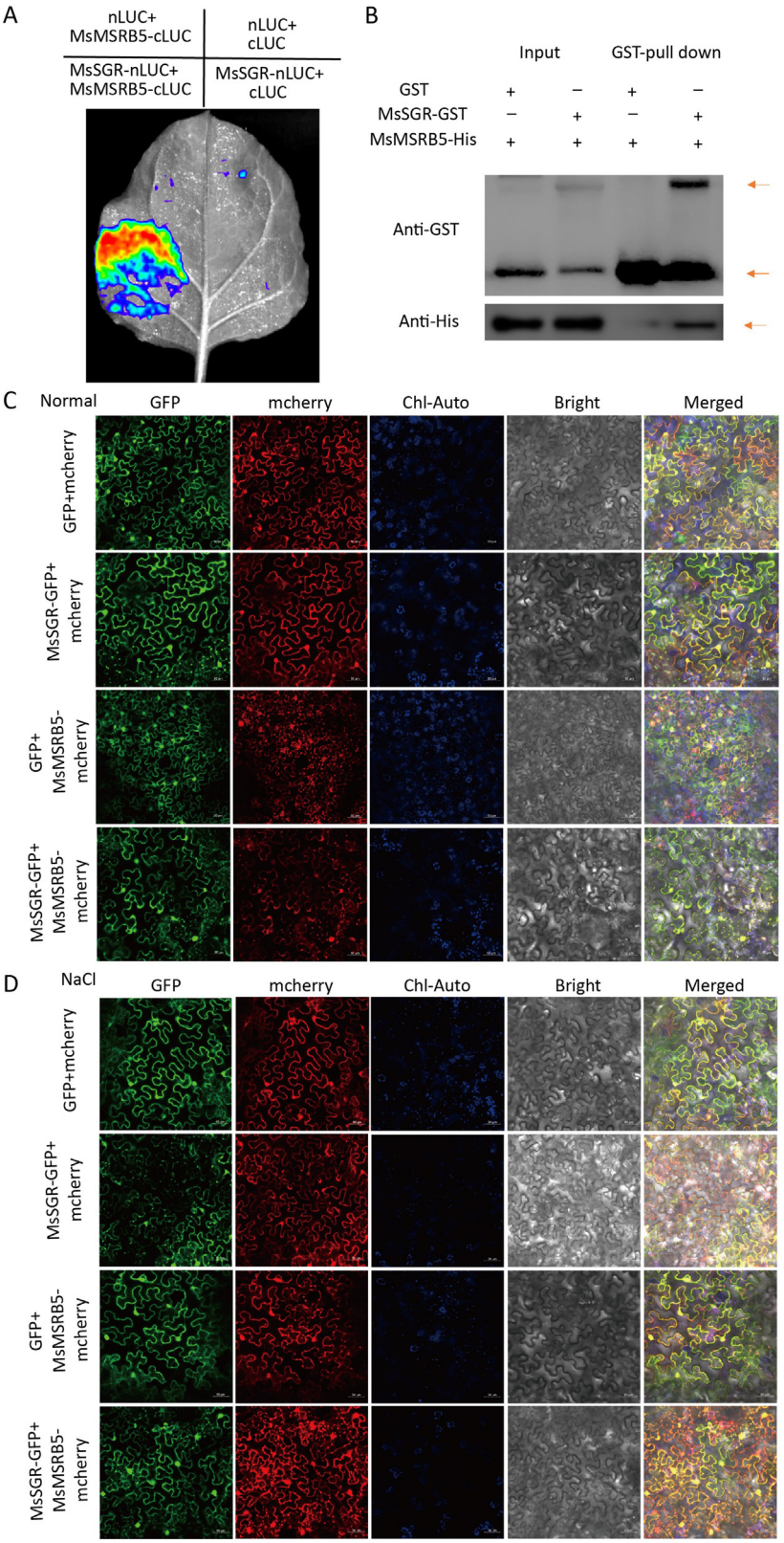


Fig. 5. Physical interactions between MsSGR and MsMSRB5. (A) Split luciferase complementation indicates an *in vivo* interaction between MsSGR and MsMSRB5 in *N. benthamiana* leaves. (B) Pull-down assay showing the interaction between MsSGR and MsMSRB5. (C, D) Subcellular localization of MsSGR and MsMSRB5 in *Nicotiana benthamiana* under control (C) and NaCl treatment (D). Green fluorescence indicates the GFP signal, red fluorescence indicates the mCherry signal, and blue fluorescence indicates the chlorophyll autofluorescence signal.

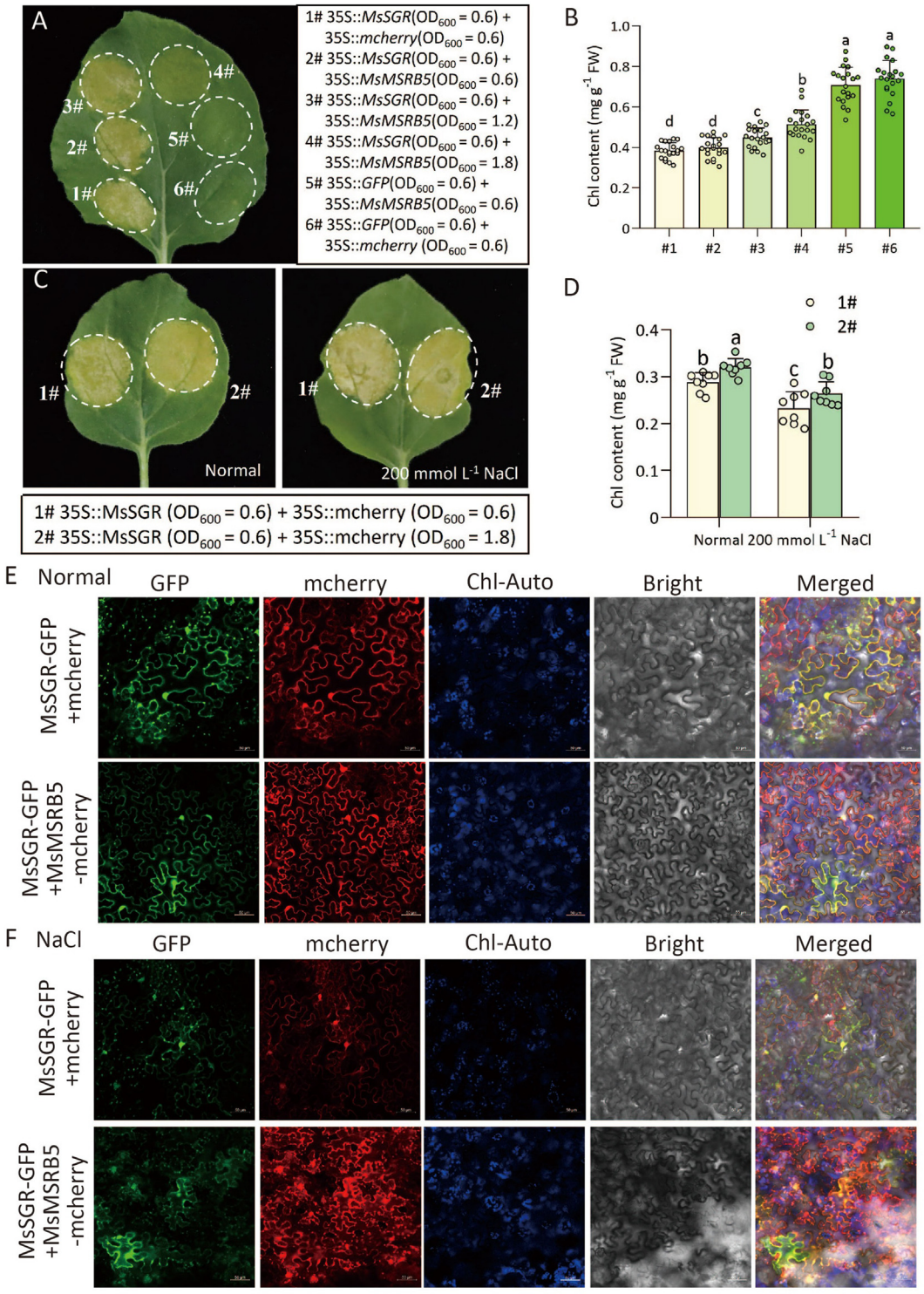


Fig. 6. MsMSRB5 inhibits MsSGR-mediated chlorophyll degradation. (A, C) Phenotypes of *Nicotiana benthamiana* leaves infiltrated with MsMSRB5 and MsSGR. (B, D) Total chlorophyll content in *Nicotiana benthamiana* leaves. Error bars indicate SD (n = 20). One-way ANOVA was performed, followed by Fisher's LSD test. Statistical significance was indicated as: $P < 0.05$ (B). Error bars indicate SD (n = 8). Two-way ANOVA was performed, followed by Fisher's LSD test. Statistical significance was indicated as: $P < 0.05$ (D). (E, F) Subcellular localization of MsSGR and MsMSRB5 in *Nicotiana benthamiana*. Green fluorescence indicates the GFP signal, red fluorescence indicates the mCherry signal, and blue fluorescence indicates the chlorophyll autofluorescence signal.

stress (Fig. 1F–H), directly impairing its photosynthetic capacity. Specifically, F_v/F_m and Y(II) decreased in *MsSGR*-OE (Fig. 2A–D). Collectively, this comprehensive decline in photosynthetic performance inhibited the growth of *MsSGR*-OE plants under salt stress (Fig. 1).

To mitigate photooxidative damage caused by excess light energy, plants dissipate redundant light energy as thermal energy via the non-photochemical quenching (NPQ) mechanism. This process usually elevates the non-photochemical quenching coefficient (q_N) [37,38]. Notably, under salt stress, *MsSGR*-OE lines exhibited

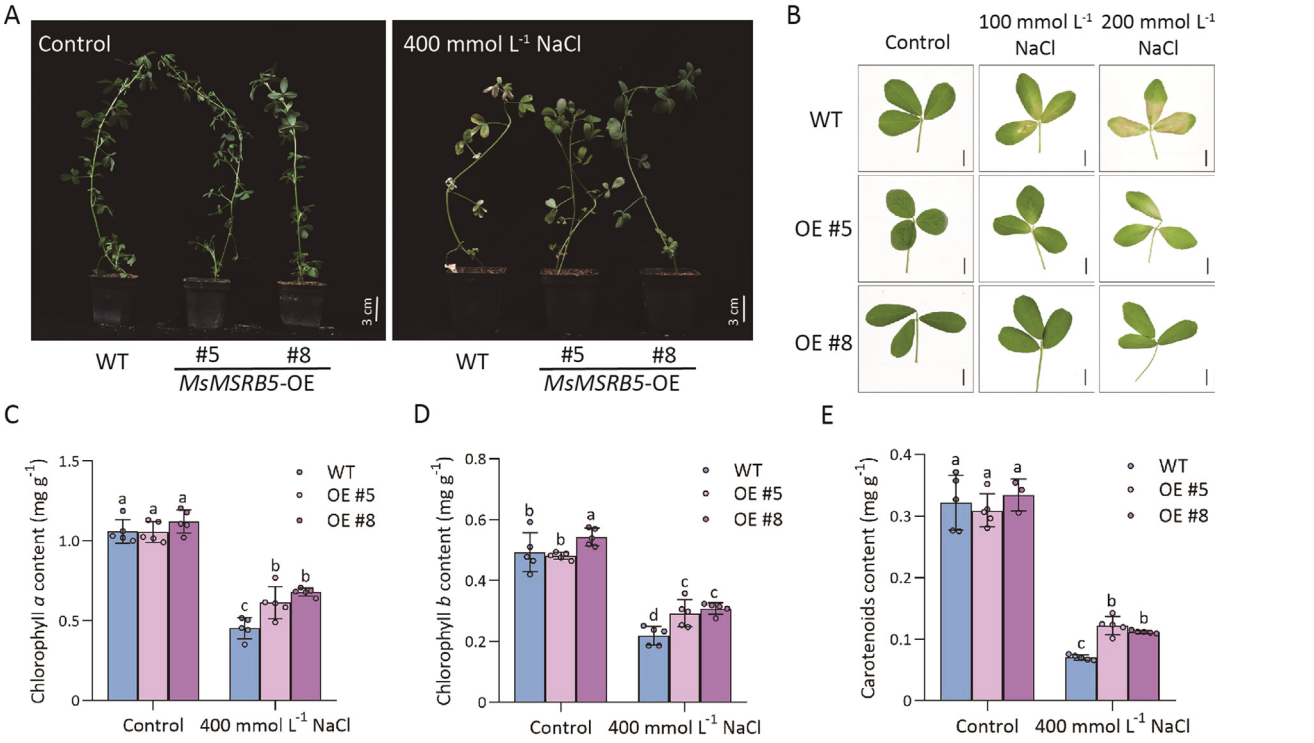


Fig. 7. *MsMSRB5*-OE enhances salt resistance in alfalfa. (A) The cuttings of WT and *MsMSRB5*-OE plants were inserted into vermiculite and cultured for 40 d, then treated with 400 mmol L^{-1} NaCl solution irrigated every two d for one week. (B) Mature leaves of WT and *MsMSRB5*-OE plants were collected at 40 d after cutting, and then immersed in nutrient solutions containing 0, 100, and 200 mmol L^{-1} NaCl for 10 d. (C) Chlorophyll *a* content in the leaves of the *MsMSRB5*-OE plants. (D) Chlorophyll *b* content in the leaves of the *MsMSRB5*-OE plants. (E) Carotenoid content in the leaves of the *MsMSRB5*-OE plants. WT, wild-type alfalfa; OE, overexpression of *MsSGR* transgenic alfalfa. Error bars indicate SD ($n = 5$). Bars labeled with different letters indicate significant differences between groups, while bars with the same letter show no significant differences (Two-way ANOVA, Fisher's LSD test, $P < 0.05$).

significantly lower NPQ/4 (Fig. 2E, F) and q_N (Fig. 2I, J) than WT, indicating that their photoprotective mechanisms have functional defects that prevent them from effectively dissipating excess light energy through the non-photochemical quenching pathway. In addition, RNA-seq analysis revealed that *MsSGR*-OE lines downregulated most DEGs enriched in several photosynthesis-related pathways, including ko00195 (Photosynthesis), ko00196 (Photosynthesis-antenna proteins), and ko00906 (Carotenoid biosynthesis) (Fig. 4). Taken together, these results demonstrate that *MsSGR*-OE exacerbates light-induced damage in alfalfa under salt stress by disrupting chlorophyll homeostasis, inhibiting the expression of photosynthetic genes, and impairing photoprotective mechanisms.

Conversely, salt-tolerant plants typically maintain higher chlorophyll levels under salt stress [35,36], which helps maintain photosynthetic efficiency and growth vitality. Consistently, the *MsSGR*-KO line exhibits enhanced photoprotective capacity under salt stress, reduces damage to photosynthetic structures, and maintains relatively stable photosynthetic capacity (Fig. S5K). *MsSGR*-KO allocates more light energy to chemical energy for photosynthesis, thus decreasing total energy dissipation, which is consistent with a previous study [39]. By optimizing energy distribution, *MsSGR*-KO protects the photosynthetic apparatus, enhances light energy utilization efficiency, and ultimately exhibits stronger photosynthetic adaptability under salt stress.

4.2. SGR modulates antioxidant responses in alfalfa under salt stress

Salt stress leads to the accumulation of ROS in plants, causing oxidative damage to cells [40–42]. ROS accumulation upregulates *SGR* expression [43], and our results further confirmed that *MsSGR* overexpression in alfalfa significantly increases H_2O_2 content during salt stress (Fig. 3E). High H_2O_2 concentrations induce lipid peroxidation, as evidenced by the elevated MDA content in the *MsSGR*-OE lines (Fig. 3C). Enzymatic and nonenzymatic antioxidants scavenge ROS. Proline is a nonenzymatic antioxidant and osmotic regulator [44] that accumulates in plants to mitigate damage from salt stress [45–47]. Interestingly, we found that the *MsSGR*-OE lines exhibited higher proline content compared with the WT under salt stress; however, high proline accumulation in *MsSGR*-OE lines did not enhance salt tolerance. In contrast, excessive proline accumulation exerts toxic effects on plant cells [48–50], a phenomenon that may have exacerbated the growth inhibition of *MsSGR*-OE lines under salt stress.

Besides nonenzymatic antioxidants, antioxidant enzymes, such as SOD and POD, play an important role in scavenging ROS and enhancing plant tolerance to abiotic stress [51,52]. For example, knocking out *ZmWRKY20* in maize [53] and overexpressing ScABI3 in alfalfa [54] enhances antioxidant enzyme activities, reduces ROS accumulation, and increases salt tolerance. Consistently, RNA sequencing and RT-qPCR studies revealed that the expression levels of key antioxidant enzyme genes (*MsSFD3*, *MsSODCP*, *MsPOD*, and *MsAPX7*) were significantly downregulated in *MsSGR*-OE lines under salt stress (Fig. 4D–G), and POD and SOD activities in *MsSGR*-OE lines were significantly lower compared with those in WT plants (Fig. 3E, F). Conversely, *MsSGR*-KO lines showed elevated POD and SOD activities (Fig. S6E, F), reduced MDA and H_2O_2 levels (Fig. S6C, E), and conferred stronger ROS scavenging and salt tolerance. Taken together, these results indicate that *MsSGR* negatively regulates salt tolerance in alfalfa by repressing the expression of antioxidant enzyme genes and the activity of antioxidant enzymes.

4.3. MsMSRB5 interacts with MsSGR and modulates plant salt tolerance

In the present study, we identified MsMSRB5 as a potential MsSGR-interacting protein through extensive Y2H screening (Fig. S7A). We further confirmed the interaction between MsSGR and MsMSRB5 in planta using split-luciferase assays and *in vitro* by pull-down experiments (Fig. 5A, B). Our gene family analysis revealed that *MsMSRB5* belongs to the *MSRB* family. The *MSRB* family enhances plant tolerance to abiotic stresses by reducing methionine sulfoxide back to methionine (Met), thereby repairing ROS-induced oxidative damage to proteins [27,55].

RT-qPCR analysis revealed that *MsMSRB5* exhibits similar tissue-specific expression patterns to *MsSGR*, with higher expression in old leaves and petioles (Fig. S15A). Subcellular localization experiment revealed that the *MsMSRB5*-mCherry fusion protein co-localized with *MsSGR*-GFP in chloroplasts and other organelles, which provides a prerequisite for the physical interaction between MsSGR and MsMSRB5 (Fig. 5). Because *MsSGR* plays an important role in chlorophyll degradation and photosynthetic pathways, we examined its transient expression in *Nicotiana benthamiana*. The results indicated that *MsMSRB5* overexpression suppressed *MsSGR*-mediated chlorophyll degradation (Fig. 6A, B). Combined with their chloroplast-localized characteristics, these results suggest that MsMSRB5 and MsSGR play key roles in chloroplast-related physiological processes, particularly in maintaining chlorophyll homeostasis.

We further confirmed that cotransformation of *MsMSRB5* and *MsSGR* during NaCl treatment suppresses *MsSGR*-induced chlorophyll degradation (Fig. 6C, D). *MsSGR* overexpression accelerated chlorophyll degradation in alfalfa (Fig. 1F–H), whereas MsMSRB5 inhibited the chlorophyll-degrading activity of MsSGR. Specifically, *MsMSRB5* overexpression increased chlorophyll content in alfalfa during salt stress (Fig. 7C–E), thereby enhancing salt tolerance.

This regulatory mechanism may also involve modulating ROS homeostasis. The MSRB family plays a conserved role in plant oxidative stress responses. For example, knocking out *AtMSRB3* in *Arabidopsis* increases H_2O_2 accumulation, whereas overexpressing *AtMSRB5* or *GsMSRB5a* reduces ROS levels in plants [29,55,56]. Chloroplasts are the primary site for ROS production in plant cells during salt stress [57,58]. We hypothesize that MsMSRB5 maintains chloroplast structural integrity by inhibiting MsSGR activity, thereby reducing excessive ROS accumulation and ultimately mitigating salt stress-induced oxidative damage; however, the specific regulatory mechanism by which MsMSRB5 and MsSGR participate in the ROS pathway warrants further study.

Taken together, we identified *MsSGR* as a key regulatory factor in the salt stress response of alfalfa. This factor negatively regulates plant salt tolerance by mediating the ROS signaling network and photosynthetic efficiency. MsMSRB5 directly inhibits MsSGR-mediated chlorophyll degradation through protein–protein interaction with MsSGR, thereby enhancing plant salt tolerance. This discovery provides potential dual target genes for genetic engineering or molecular breeding of salt-tolerant alfalfa cultivars and lays a theoretical foundation for subsequent stress-resistant breeding practices.

CRediT authorship contribution statement

Chun Li: Writing – review & editing, Writing – original draft, Software, Project administration, Methodology, Investigation, Data curation, Conceptualization. **Xiaoxia Shen:** Writing – review & editing, Supervision, Project administration, Formal analysis. **Yulin Jing:** Software, Investigation, Data curation. **Ziyi Hao:** Investigation, Data curation. **Rongchen Yang:** Writing – review & editing. **Jiahua Wu:** Software, Formal analysis. **Jie An:** Writing – review & editing. **Peizhi Yang:** Supervision, Project administration, Funding acquisition, Conceptualization.

Declaration of competing interest

The authors declare that they have no known competing financial interests or personal relationships that could have appeared to influence the work reported in this paper.

Acknowledgments

This work was supported by the China Agriculture Research System of MOF and MARA, and the Biological Breeding-National Science and Technology Major Project (2022ZD04011).

Appendix A. Supplementary data

Supplementary data for this article can be found online at https://doi.org/10.1016/j.cj.2026.03.016.

References

[1] J. Du, H. Xu, D. Zhang, S. Feng, Chelation and nanoparticle delivery of monomeric dopamine to increase plant salt stress resistance, Nat. Commun. 16 (2025) 14.
[2] E. van Zelm, Y. Zhang, C. Testerink, Salt tolerance mechanisms of plants, Annu. Rev. Plant Biol. 71 (2020) 403–433.
[3] S.V. Isayenkov, F.J.M. Maathuis, Plant salinity stress: many unanswered questions remain, Front. Plant Sci. 10 (2019) 80.
[4] R. Munns, M. Tester, Mechanisms of salinity tolerance, Annu. Rev. Plant Biol. 59 (2008) 651–681.
[5] S.J. Roy, S. Negrao, M. Tester, Salt resistant crop plants, Curr. Opin. Biotechnol. 26 (2014) 115–124.
[6] C. Zoerb, C.M. Geilfus, K.J. Dietz, Salinity and crop yield, Plant Biol. 21 (2019) 31–38.
[7] I. Armstead, I. Donnison, S. Aubry, J. Harper, S. Hortensteiner, C. James, J. Mani, M. Moffet, H. Ougham, L. Roberts, A. Thomas, N. Weeden, H. Thomas, I. King, Cross-species identification of Mendel's/locus, Science 315 (2007) 73.
[8] C.S. Barry, R.P. Mcquinn, M. Chung, A. Besuden, J.J. Giovannoni, Amino acid substitutions in homologs of the STAY-GREEN protein are responsible for the green-flesh and chlorophyll retainer mutations of tomato and pepper, Plant Physiol. 147 (2008) 179–187.
[9] C. Fang, C. Li, W. Li, Z. Wang, Z. Zhou, Y. Shen, M. Wu, Y. Wu, G. Li, L. Kong, C. Liu, S.A. Jackson, Z. Tian, Concerted evolution of D1 and D2 to regulate chlorophyll degradation in soybean, Plant J. 77 (2014) 700–712.
[10] C. Zhou, L. Han, C. Pislariu, J. Nakashima, C. Fu, Q. Jiang, L. Quan, E.B. Blancaflor, Y. Tang, J.H. Bouton, M. Udvardi, G. Xia, Z. Wang, From model to crop: functional analysis of a *STAY-GREEN* gene in the model legume *Medicago truncatula* and effective use of the gene for alfalfa improvement, Plant Physiol. 157 (2011) 1483–1496.
[11] Y. Shimoda, H. Ito, A. Tanaka, *Arabidopsis STAY-GREEN*, mendel's green cotyledon gene, encodes magnesium-dechelatase, Plant Cell 28 (2016) 2147–2160.
[12] Y. Sakuraba, S. Park, Y. Kim, S. Wang, S. Yoo, S. Hoertensteiner, N. Paek, *Arabidopsis STAY-GREEN2* is a negative regulator of chlorophyll degradation during leaf senescence, Mol. Plant 7 (2014) 1288–1302.
[13] S. Park, J. Yu, J. Park, J. Li, S. Yoo, N. Lee, S. Lee, S. Jeong, H.S. Seo, H. Koh, J. Jeon, Y. Park, N. Paek, The senescence-induced stay green protein regulates chlorophyll degradation, Plant Cell 19 (2007) 1649–1664.
[14] J. Zhang, H. Li, X. Huang, J. Xing, J. Yao, T. Yin, J. Jiang, P. Wang, B. Xu, *STAYGREEN*-mediated chlorophyll *a* catabolism is critical for photosystem stability during heat-induced leaf senescence in perennial ryegrass, Plant Cell Environ. 45 (2022) 1412–1427.
[15] R.G. Bade, M.L. Bao, W.Y. Jin, Y. Ma, A. Hasi, Genome-wide identification and analysis of the *SGR* gene family in *Cucumis melo* L., Genet. Mol. Res. 15 (2016), https://doi.org/10.4238/gmr15048485.
[16] Z. Luo, J. Zhang, J. Li, C. Yang, T. Wang, B. Ouyang, H. Li, J. Giovannoni, Z. Ye, A STAY-GREEN protein SlSGR1 regulates lycopene and β-carotene accumulation by interacting directly with SlPSY1 during ripening processes in tomato, New Phytol. 198 (2013) 442–452.
[17] Y. Sakuraba, D. Kim, Y. Kim, S. Hoertensteiner, N. Paek, *Arabidopsis STAYGREEN-LIKE* (*SGRL*) promotes abiotic stress-induced leaf yellowing during vegetative growth, FEBS Lett. 588 (2014) 3830–3837.
[18] S. Black, E.M. Harte, B. Hudson, L. Wartofsky, A specific enzymatic reduction of l (-) methionine sulfoxide and a related nonspecific reduction of disulfides, J. Biol. Chem. 235 (1960) 2910–2916.

[19] E. Chatelain, P. Satour, E. Laugier, B.L. Vu, N. Payet, P. Rey, F. Montrichard, Evidence for participation of the methionine sulfoxide reductase repair system in plant seed longevity, Proc. Natl. Acad. Sci. U. S. A. 110 (2013) 3633–3638.
[20] A. Hazra, V. Varshney, P. Verma, N.U. Kamble, S. Ghosh, R.K. Achary, S. Gautam, M. Majee, Methionine sulfoxide reductase B5 plays a key role in preserving seed vigor and longevity in rice (*Oryza sativa*), New Phytol. 236 (2022) 1042–1060.
[21] E. Laugier, L. Tarrago, C.V.D. Santos, F. Eymery, M. Havaux, P. Rey, *Arabidopsis thaliana* plastidial methionine sulfoxide reductases B, MSRBs, account for most leaf peptide MSR activity and are essential for growth under environmental constraints through a role in the preservation of photosystem antennae, Plant J. 61 (2010) 271–282.
[22] S. Lee, C. Li, K.W. Koh, H. Chuang, Y. Chen, C. Lin, M. Chan, MSRB7 reverses oxidation of GSTF2/3 to confer tolerance of *Arabidopsis thaliana* to oxidative stress, J. Exp. Bot. 65 (2014) 5049–5062.
[23] S. Roy, A.K. Nandi, *Arabidopsis thaliana* methionine sulfoxide reductase B8 influences stress-induced cell death and effector-triggered immunity, Plant Mol. Biol. 93 (2017) 109–120.
[24] S. Jacques, B. Ghesquiere, P. De Bock, H. Demol, K. Wahni, P. Willems, J. Messens, F. Van Breusegem, K. Gevaert, Protein methionine sulfoxide dynamics in *Arabidopsis thaliana* under oxidative stress, Mol. Cell. Proteomics 14 (2015) 1217–1229.
[25] J. Zhu, P. Ding, Q. Li, Y. Gao, F. Chen, G. Xia, Molecular characterization and expression profile of methionine sulfoxide reductase gene family in maize (*Zea mays*) under abiotic stresses, Gene 562 (2015) 159–168.
[26] X. Guo, Y. Wu, Y. Wang, Y. Chen, C. Chu, OsMSRA4.1 and OsMSRB1.1, two rice plastidial methionine sulfoxide reductases, are involved in abiotic stress responses, Planta 230 (2009) 227–238.
[27] C. Li, S. Lee, P. Chieh, C. Lin, Y. Wang, M. Chan, *Arabidopsis* root-abundant cytosolic methionine sulfoxide reductase b genes *MsrB7* and *MsrB8* are involved in tolerance to oxidative stress, Plant Cell Physiol. 53 (2012) 1707–1719.
[28] T. Xiao, M. Mi, C. Wang, M. Qian, Y. Chen, L. Zheng, H. Zhang, Z. Hu, Z. Shen, Y. Xia, A methionine-R-sulfoxide reductase, OsMSRB5, is required for rice defense against copper toxicity, Environ. Exp. Bot. 153 (2018) 45–53.
[29] X. Sun, M. Sun, B. Jia, Z. Qin, K. Yang, C. Chen, Q. Yu, Y. Zhu, A *Glycine soja* methionine sulfoxide reductase B5a interacts with the Ca^{2+}/CAM-binding kinase GsCBRLK and activates ROS signaling under carbonate alkaline stress, Plant J. 86 (2016) 514–529.
[30] H. Chen, Y. Zou, Y. Shang, H. Lin, Y. Wang, R. Cai, X. Tang, J. Zhou, Firefly luciferase complementation imaging assay for protein-protein interactions in plants, Plant Physiol. 146 (2008) 368–376.
[31] C. Chen, H. Chen, Y. Zhang, H.R. Thomas, M.H. Frank, Y. He, R. Xia, TBtools: an integrative toolkit developed for interactive analyses of big biological data, Mol. Plant 13 (2020) 1194–1202.
[32] K. Tamura, G. Stecher, S. Kumar, MEGA11 molecular evolutionary genetics analysis version 11, Mol. Biol. Evol. 38 (2021) 3022–3027.
[33] M.A. Shahid, A. Sarkhosh, N. Khan, R.M. Balal, S. Ali, L. Rossi, C. Gomez, N. Mattson, W. Nasim, F. Garcia-Sanchez, Insights into the physiological and biochemical impacts of salt stress on plant growth and development, Agronomy 10 (2020) 938.
[34] Z. Li, S. Wu, J. Chen, X. Wang, J. Gao, G. Ren, B. Kuai, NYEs/SGRs-mediated chlorophyll degradation is critical for detoxification during seed maturation in *Arabidopsis*, Plant J. 92 (2017) 650–661.
[35] Y. Luan, Z. Chen, Z. Fang, X. Huang, D. Zhao, J. Tao, PoWRKY71 is involved in *Paeonia ostii* resistance to drought stress by directly regulating light-harvesting chlorophyll *a*/*b*-binding 151 gene, Hortic. Res. 10 (2023) 194.
[36] T. Wang, J. Yang, J. Cao, Q. Zhang, H. Liu, P. Li, Y. Huang, W. Qian, X. Bi, H. Wang, Y. Zhang, MsbZIP55 regulates salinity tolerance by modulating melatonin biosynthesis in alfalfa, Plant Biotechnol. J. 23 (2025) 2125–2139.
[37] Z. Ali, Y. Sun, Z. Ma, Y. Zheng, Y. Liu, VvHY5 and VvBEE1 antagonistically control resveratrol biosynthesis to mitigate high light-induced damage in grapevine, J. Integr. Plant Biol. 67 (2025) 993–1008.
[38] A. Li, T. You, X. Pang, Y. Wang, L. Tian, X. Li, Z. Liu, Structural basis for an early stage of the photosystem II repair cycle in *Chlamydomonas reinhardtii*, Nat. Commun. 15 (2024) 17.
[39] D. Shevela, J.F. Kern, G. Govindjee, J. Messinger, Solar energy conversion by photosystem II: principles and structures, Photosynth. Res. 156 (2023) 279–307.
[40] Y. Li, F. Jiang, Z. He, Y. Liu, Z. Chen, C. Ottosen, R. Mittler, Z. Wu, R. Zhou, Higher intensity of salt stress accompanied by heat inhibits stomatal conductance and induces ROS accumulation in tomato plants, Antioxidants 13 (2024) 448.
[41] E. Schmid-Siegert, O. Stepushenko, G. Glauser, E.E. Farmer, Membranes as structural antioxidants recycling of malondialdehyde to its source in oxidation-sensitive chloroplast fatty acids, J. Biol. Chem. 291 (2016) 13005–13013.
[42] A. Choudhary, A. Kumar, N. Kaur, ROS and oxidative burst: roots in plant development, Plant Divers. 42 (2020) 33–43.
[43] Y.Y. Peng, L.L. Liao, S. Liu, M.M. Nie, J. Li, L.D. Zhang, J.F. Ma, Z.C. Chen, Magnesium deficiency triggers SGR-mediated chlorophyll degradation for magnesium remobilization, Plant Physiol. 181 (2019) 262–275.
[44] C.B. Chen, M.B. Dickman, Proline suppresses apoptosis in the fungal pathogen *Colletotrichum trifolii*, Proc. Natl. Acad. Sci. U. S. A. 102 (2005) 3459–3464.
[45] A.E. Moukhtari, C. Cabassa-Hourton, M. Farissi, A. Savoure, How does proline treatment promote salt stress tolerance during crop plant development?, Front. Plant Sci. 11 (2020) 1127.
[46] J. Yang, L. Qiu, Q. Mei, Y. Sun, N. Li, X. Gong, F. Ma, K. Mao, MdHB7-like positively modulates apple salt tolerance by promoting autophagic activity and Na^+ efflux, Plant J. 116 (2023) 669–689.
[47] A. Siddique, G. Kandpal, P. Kumar, Proline accumulation and its defensive role under diverse stress condition in plants: an overview, J. Pure Appl. Microbiol. 12 (2018) 1655–1659.
[48] S. Hayat, Q. Hayat, M.N. Alyemeni, A.S. Wani, J. Pichtel, A. Ahmad, Role of proline under changing environments, Plant Signal. Behav. 7 (2012) 1456–1466.
[49] B. Heuer, Influence of exogenous application of proline and glycinebetaine on growth of salt-stressed tomato plants, Plant Sci. 165 (2003) 693–699.
[50] D. Roy, N. Basu, A. Bhunia, S. Banerjee, Counteraction of exogenous l-proline with NaCl in salt-sensitive cultivar of rice, Biol. Plant. 35 (1993) 69–72.
[51] C. Niu, L. Jiang, F. Cao, C. Liu, J. Guo, Z. Zhang, Q. Yue, N. Hou, Z. Liu, X. Li, M.M. Tahir, J. He, Z. Li, C. Li, F. Ma, Q. Guan, Methylation of a MITE insertion in the *MdRFNR1-1* promoter is positively associated with its allelic expression in apple in response to drought stress, Plant Cell 34 (2022) 3983–4006.
[52] Q. Ye, L. Zheng, P. Liu, Q. Liu, T. Ji, J. Liu, Y. Gao, L. Liu, J. Dong, T. Wang, The S-acylation cycle of transcription factor *MtNAC80* influences cold stress responses in *Medicago truncatula*, Plant Cell 36 (2024) 2629–2651.
[53] C. Bo, R. Cai, X. Fang, H. Wu, Z. Ma, H. Yuan, B. Cheng, J. Fan, Q. Ma, Transcription factor ZmWRKY20 interacts with ZmWRKY115 to repress expression of ZmbZIP111 for salt tolerance in maize, Plant J. 111 (2022), 1660–1675.
[54] Y. Zhang, Y. Zhang, C. Wang, J. Xiao, M. Huang, L. Zhuo, D. Zhang, Enhancement of salt tolerance of alfalfa: physiological and molecular responses of transgenic alfalfa plants expressing *Syntrichia caninervis*-derived ScABI3, Plant Physiol. Biochem. 207 (2024) 108335.
[55] Y. Cai, J. Cai, J. Lee, Y. Li, F.K. Balladona, D. Sukma, M. Chan, *Arabidopsis AtMSRB5* functions as a salt-stress protector for both *Arabidopsis* and rice, Front. Plant Sci. 14 (2023) 1072173.
[56] S.J. Kwon, S.I. Kwon, M.S. Bae, E.J. Cho, O.K. Park, Role of the methionine sulfoxide reductase MsrB3 in cold acclimation in *Arabidopsis*, Plant Cell Physiol. 48 (2007) 1713–1723.
[57] W. Xu, H. Lv, M. Zhao, Y. Li, Y. Qi, Z. Peng, G. Xia, M. Wang, Proteomic comparison reveals the contribution of chloroplast to salt tolerance of a wheat introgression line, Sci. Rep. 6 (2016) 32384.
[58] Y. Zhuang, M. Wei, C. Ling, Y. Liu, A.K. Amin, P. Li, P. Li, X. Hu, H. Bao, H. Huo, J. Smalle, S. Wang, EGY3 mediates chloroplastic ROS homeostasis and promotes retrograde signaling in response to salt stress in *Arabidopsis*, Cell Rep. 36 (2021) 109384.